

# FTIR Microscopy with Polarized IR Radiation for the Analysis of SAPO-5 and *p*-Xylene-Loaded SAPO-5

F. Schüth,<sup>\*,†</sup> D. Demuth,<sup>†</sup> B. Zibrowius,<sup>‡</sup> J. Kornatowski,<sup>§</sup> and G. Finger<sup>||</sup>

Contribution from the Institut für Anorganische Chemie und Analytische Chemie der Johannes Gutenberg-Universität Mainz, W-6500 Mainz, Germany, University of Manchester Institute of Science and Technology, Manchester, M601QD England, Institut für Kristallographie der Johann-Wolfgang-Goethe-Universität Frankfurt, W-6000 Frankfurt, Germany, and Zentrum für Heterogene Katalyse, O-1199 Berlin, Germany

Received June 7, 1993<sup>⊙</sup>

**Abstract:** Using an optimized procedure, large SAPO-5 single crystals (up to 250 × 75 μm) with a very high optical quality could be synthesized. NMR spectroscopy proved the perfect incorporation of silicon on phosphorus sites. IR microscopy with polarized IR radiation revealed that both types of OH groups, with absorption bands at 3627 and 3519 cm<sup>-1</sup>, are oriented almost perpendicularly to the crystal *c*-axis, thus protruding into the 12-membered and the 6-membered ring channels, respectively. Adsorbed *p*-xylene reacts with both types of OH groups, giving rise to one broad band for the OH vibration at 3233 cm<sup>-1</sup>, which indicates a shift of the proton from the 6-membered ring to the 12-membered ring. From the dichroic ratios of the bands due to the *p*-xylene, it can be inferred that the long axis of the *p*-xylene molecule is oriented parallel to the channel axis of the molecular sieve.

## Introduction

The materials of the AlPO<sub>4</sub> family and their isomorphously substituted derivatives, for instance, the SAPOs have attracted considerable interest since their discovery in the early 1980s by the pioneering work of the group led by E. Flanigen.<sup>1,2</sup> One of the recent interesting applications, developed by G. D. Stucky and his co-workers, is the use of AlPO<sub>4</sub>-5 as a host matrix for *p*-nitroaniline<sup>3-5</sup> which resulted in a strong second-harmonic generation (SHG) due to the ordering of the *p*-nitroaniline in the AlPO<sub>4</sub>-5 channel system. J. Caro and his group went one step further and investigated the SHG from a *p*-nitroaniline-loaded single crystal of AlPO<sub>4</sub>-5 which could be oriented with respect to the incident laser beam.<sup>6,7</sup> They found the strongest SHG signal for the crystal oriented with its long axis (direction of the unidimensional channel system) in the polarization plane of the incident laser beam and almost no signal for the crystal oriented perpendicular to the polarization plane. This suggests, that the *p*-nitroaniline molecules are very well aligned by the channel system of the microporous host.

One decisive prerequisite for optical applications, for instance SHG of host/guest systems based on microporous host crystals, however, is a very high quality of the crystals employed. On the one hand, the crystals have to be large enough to be studied as single crystals; on the other hand, the optical quality has to be sufficiently high. Procedures for synthesizing large AlPO<sub>4</sub>-5 and SAPO-5 crystals have been described in the literature.<sup>8-11</sup> Crystals

prepared following this procedure are almost perfect in shape and are usually obtained as single crystals. However, under the optical microscope, they appear inhomogeneous, an effect which is not observed when the crystals are analyzed by SEM, which is the usual method. These inhomogeneities lead to highly undesirable scattering losses in optical studies and render future applications of such materials difficult. Moreover, due to these scattering losses, it has not been possible, as yet, to obtain decent IR spectra of AlPO<sub>4</sub>-5 or SAPO-5 single crystals, as had previously been possible for silicalite I.<sup>12</sup>

In this study we will report on the synthesis of optically perfect single crystals of SAPO-5 up to 250-μm long and polarized infrared spectra of these crystals. In addition, the crystals were loaded in situ with *p*-xylene, using a newly constructed high-vacuum cell for the IR microscope, and analyzed subsequently with polarized IR radiation. *p*-Xylene was chosen as the adsorbate for four reasons: (1) It can serve as a model substance, since many of the molecules exhibiting nonlinear optical properties have the same elongated shape.<sup>13</sup> (2) It is relatively easy to handle, whereas the materials which actually exhibit strong NLO properties would severely contaminate the high-vacuum cell. (3) Comparison with the previous study of *p*-xylene in silicalite I is possible. (4) Reaction of the weakly basic molecule *p*-xylene with the acidic OH groups of the SAPO allows inferences on the acidic properties of SAPO-5.

## Experimental Section

**Synthesis.** The synthesis was similar to the one described by Finger and Kornatowski.<sup>14</sup> This system was optimized with respect to optically homogeneous crystals by varying the raw materials, reaction conditions, and experimental procedures. An optimized synthesis mixture had the formal molar composition Al<sub>2</sub>O<sub>3</sub>:P<sub>2</sub>O<sub>5</sub>:SiO<sub>2</sub>:triethylamine:H<sub>2</sub>O = 1:1.03:0.15:1.55:750. The gel was prepared according to the following

<sup>†</sup> Universität Mainz.

<sup>‡</sup> University of Manchester Institute of Science and Technology.

<sup>§</sup> Universität Frankfurt.

<sup>||</sup> Zentrum für Heterogene Katalyse.

⊙ Abstract published in *Advance ACS Abstracts*, December 15, 1993.

(1) Wilson, S. T.; Lok, B. M.; Messina, C. A.; Cannan, T. R.; Flanigen, E. M. *J. Am. Chem. Soc.* **1982**, *104*, 1146-7.

(2) Lok, B. M.; Messina, C. A.; Patton, R. L.; Cannan, T. R.; Flanigen, E. M. *J. Am. Chem. Soc.* **1984**, *106*, 6092-3.

(3) Cox, S. D.; Gier, T. E.; Stucky, G. D. *Chem. Mater.* **1990**, *2*, 609-19.

(4) Cox, S. D.; Gier, T. E.; Stucky, G. D.; Bierlein, J. *J. Am. Chem. Soc.* **1988**, *110*, 2986-8.

(5) Cox, S. D.; Gier, T. E.; Stucky, G. D.; Bierlein, J. *Solid State Ionics* **1989**, *32/33*, 514-20.

(6) Werner, L.; Caro, J.; Finger, G.; Kornatowski, J. *Zeolites* **1992**, *12*, 659-71.

(7) Caro, J.; Finger, G.; Kornatowski, J.; Richter-Mendau, J.; Werner, J.; Zibrowius, B. *Adv. Mater.* **1992**, *4*, 273-6.

(8) Finger, G.; Kornatowski, J. *Zeolites* **1990**, *10*, 615-7.

(9) Kornatowski, J.; Finger, G. *Bull. Soc. Chim. Belg.* **1990**, *99*, 857-9.

(10) Finger, G.; Richter-Mendau, J.; Bülow, M.; Kornatowski, J. *Zeolites* **1991**, *11*, 443-8.

(11) Finger, G.; Kornatowski, J.; Richter-Mendau, J.; Jancke, K.; Bülow, M.; Rozwadowski, M. *Stud. Surf. Sci. Catal.* **1991**, *65*, 501-9.

(12) Schüth, F. *J. Phys. Chem.* **1992**, *96*, 7493-6.

(13) See, for instance: Twieg, R. J.; Kanti, J. In *Nonlinear Optical Properties of Organic and Polymeric Materials*; Williams, D. J., Ed.; ACS Symposium Series 233; American Chemical Society: Washington, DC, 1983; pp 57-69.

(14) Finger, G.; Kornatowski, J. *Zeolites* **1990**, *10*, 615-7.

Table 1. Experimental Conditions for MAS NMR Measurements

nucleus	resonance frequency (MHz)	pulse duration ( $\mu$ s)	flip angle	repetition time (s)	MAS frequency (kHz)	no. of scans	external reference
$^{29}\text{Si}$	79.5	2.5	$\pi/4$	5.0	4.2	>2000	TMS
$^{27}\text{Al}$	104.2	0.6	$\pi/12$	0.5	15.0	800	$\text{Al}(\text{H}_2\text{O})_6^{3+}$
$^{31}\text{P}$	161.9	3.0	$\pi/2$	15.0	15.0	64	$\text{H}_3\text{PO}_4$ , 85 wt %

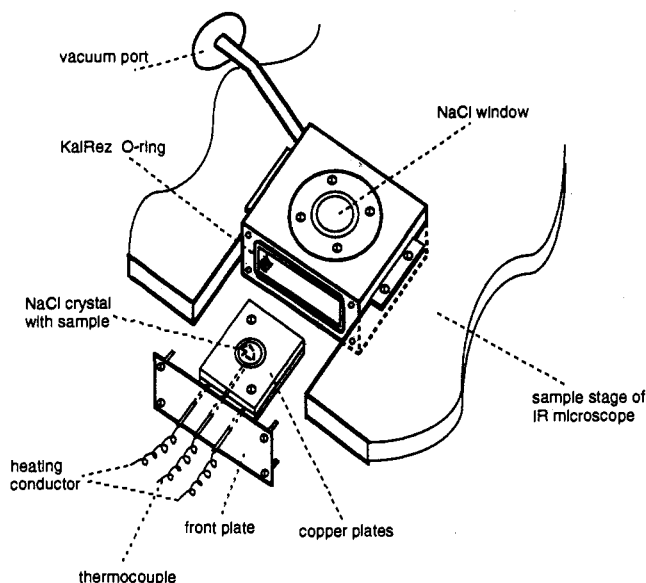


Figure 1. Schematic drawing of HV cell for the IR microscope.

procedure: Solution A was prepared by adding triethylamine (Aldrich, 99%) dropwise into ice-cooled  $\text{H}_3\text{PO}_4$  (orthophosphoric acid, Merck, 85%) while stirring. The final pH of this solution was 2.5. Solution B was formed from pyrogenic silica (Aerosil 200, DEGUSSA) which was reacted with the aluminum source (aluminumoxidehydrate sol, 1.7%  $\text{Al}_2\text{O}_3$  by AAS, pH 5.8, CTA Säureschutz, Berlin) for 2 h under vigorous stirring, resulting in a solution with a pH of 6.5. Solution A was added dropwise into solution B over a period of 10 min, followed by a final stirring period of 15 min. The pH of the final gel was 3.0. The reaction mixture was filled in a Teflon-lined stainless steel autoclave (Berghoff, DABII, 50 mL) and then placed in a preheated heating block, resulting in a fast temperature increase to the final temperature of 483 K. After crystallization at this temperature for 70 h, the autoclave was quenched and the product separated by decantation, washed, and dried at 393 K overnight. It should be noted here that deviations from this procedure, especially the use of different  $\text{SiO}_2$  or  $\text{Al}_2\text{O}_3$  sources, resulted in crystals with an appreciably lower quality.

To remove the template, the crystals were calcined in air by heating to 523 K with a rate of 1 K/min and keeping them there for 2 h. Then the temperature was further raised to 923 K at 1 K/min and the crystals were calcined at this temperature for 10 h. After this calcination procedure the crystals were absolutely clear and colorless.

**MAS NMR Measurements.** The  $^{27}\text{Al}$ ,  $^{29}\text{Si}$ , and  $^{31}\text{P}$  MAS NMR spectra were recorded on a Bruker MSL 400 spectrometer. The experimental conditions are given in Table 1 and were identical to those given in ref 15 except that for  $^{27}\text{Al}$  and  $^{31}\text{P}$  a higher spinning rate of 15 kHz was used. All spectra were obtained by single-pulse excitation for the calcined sample dehydrated for at least 3 h at 400 K prior to the measurement.

**IR Measurements.** The IR measurements were carried out using a SpectraTec Research Plan microscope attached to a Nicolet 5SXB-E optical bench. Polarization was achieved by use of a ZnSe wire grid polarizer. Depolarization of the IR radiation by the objective, the sample cell, and the condenser was checked with a second polarizer placed below the condenser and found to be less than 5%. For recording spectra the sample was placed on a NaCl crystal in a high-vacuum cell which itself was mounted into the sample stage of the microscope, Figure 1.

The body of the cell is made of stainless steel into which two NaCl windows are fitted and sealed with KalRez O-rings. The system is pumped by a turbomolecular pump with a dosing system integrated into the pumping line. Pressure is recorded using a Pirani gauge. The NaCl crystal which supports the sample is held between two copper plates. The

copper plates are heated by a metal mantled heating conductor. The temperature is measured by a thermocouple contacting the NaCl crystal. Temperature is controlled by a Eurotherm 818 P PID controller. The whole sample holder is attached to the removable front plate of the cell and is sealed to the cell by KalRez O-rings.

The vacuum which can be achieved in this cell is better than the lower limit of the Pirani gauge ( $<10^{-3}$  Torr). At this pressure the sample holder can be heated to 750 K without damage to the cell.

For the IR measurements several crystals were placed on the sample holder and a crystal oriented in either the north-south or east-west direction was selected by means of two adjustable rectangular apertures above and below the sample. To remove adsorbed water, the samples were activated in situ prior to measurement by heating them to 473 K with a rate of 10 K/min and keeping them at this temperature for 90 min under high vacuum,  $<10^{-3}$  Torr. This was usually sufficient to remove all water as was observed by IR measurements.

Loading of *p*-xylene was carried out in situ after activation of the samples at a *p*-xylene pressure of 4.5 Torr and a temperature of 373 K over a period of 5–10 h. The SAPO-5 crystals were exposed to *p*-xylene until the absorbance of *p*-xylene bands in the IR spectra had reached a constant value, indicating saturation of the samples.

## Results

Using the synthesis procedure outlined in the Experimental Section, it is possible to synthesize SAPO-5 crystals which exhibit a perfect morphology (SEM, Figure 2 (top)) and are of high optical quality (optical microscope, Figure 2 (bottom)). The crystals are completely transparent, as one can see the underlying crystal in the micrograph almost without any distortion. Also in polarized visible light the crystals are completely homogeneous. The  $^{27}\text{Al}$  and  $^{31}\text{P}$  MAS NMR spectra agree with those previously obtained for dehydrated calcined  $\text{AlPO}_4$ -5 and SAPO-5.<sup>15–18</sup> The lines at 35.5 ppm ( $^{27}\text{Al}$ ) and  $-30.3$  ppm ( $^{31}\text{P}$ ) are characteristic of  $\text{Al}(\text{OP})_4$  and  $\text{P}(\text{OAl})_4$  environments, respectively.  $^{29}\text{Si}$  MAS NMR spectroscopy is the only direct method to check the incorporation of silicon into an aluminophosphate framework. The  $^{29}\text{Si}$  MAS NMR spectrum in Figure 3 shows that almost all silicon ( $>90\%$ ) present in the sample under study is incorporated on phosphorus sites in the AFI framework. The intense line at  $-95.6$  ppm is characteristic of  $\text{Si}(\text{OAl})_4$  groups in silicoaluminophosphates.<sup>16,19</sup> This type of silicon incorporation generates one Brønsted acid site per silicon and was found to be predominant for SAPO-5 synthesized in a similar way as in the above outlined synthesis procedure.<sup>16,18</sup> The minor line at about  $-110$  ppm can be assigned to  $\text{Si}(\text{OSi})_4$  groups present in "silica patches" in the AFI framework and/or in a very small amount of amorphous silica.<sup>16,17</sup>

The high quality of the crystals is the prerequisite for the recording of sufficiently noise-free IR spectra of SAPO-5 single crystals. Several previous attempts to obtain good spectra had failed because almost no energy was monitored at the detector when studying SAPO-5 or  $\text{AlPO}_4$ -5 crystals, due to the large scattering losses and reflexion losses from the crystal faces not perpendicular to the incident IR beam.

As Figure 4 shows, this is different for the crystals synthesized and investigated here. Polarized spectra of a SAPO-5 single crystal which had been evacuated at a pressure below  $10^{-3}$  Torr

(16) Goepper, M.; Guth, F.; Delmotte, L.; Guth, J. L.; Kessler, H. *Stud. Surf. Sci. Catal.* **1989**, *49*, 857–66.

(17) Martens, J. A.; Mertens, M.; Grobet, P. J.; Jacobs, P. A. *Stud. Surf. Sci. Catal.* **1988**, *37*, 97–105.

(18) Zibrowius, B.; Löffler, E.; Finger, G.; Sonntag, E.; Hunger, M.; Kornatowski, J. *Stud. Surf. Sci. Catal.* **1991**, *65*, 537–48.

(19) Blackwell, C. S.; Patton, R. L. *J. Phys. Chem.* **1988**, *92*, 3965–70.

(15) Zibrowius, B.; Loeffler, E.; Hunger, M. *Zeolites* **1992**, *12*, 167–74.

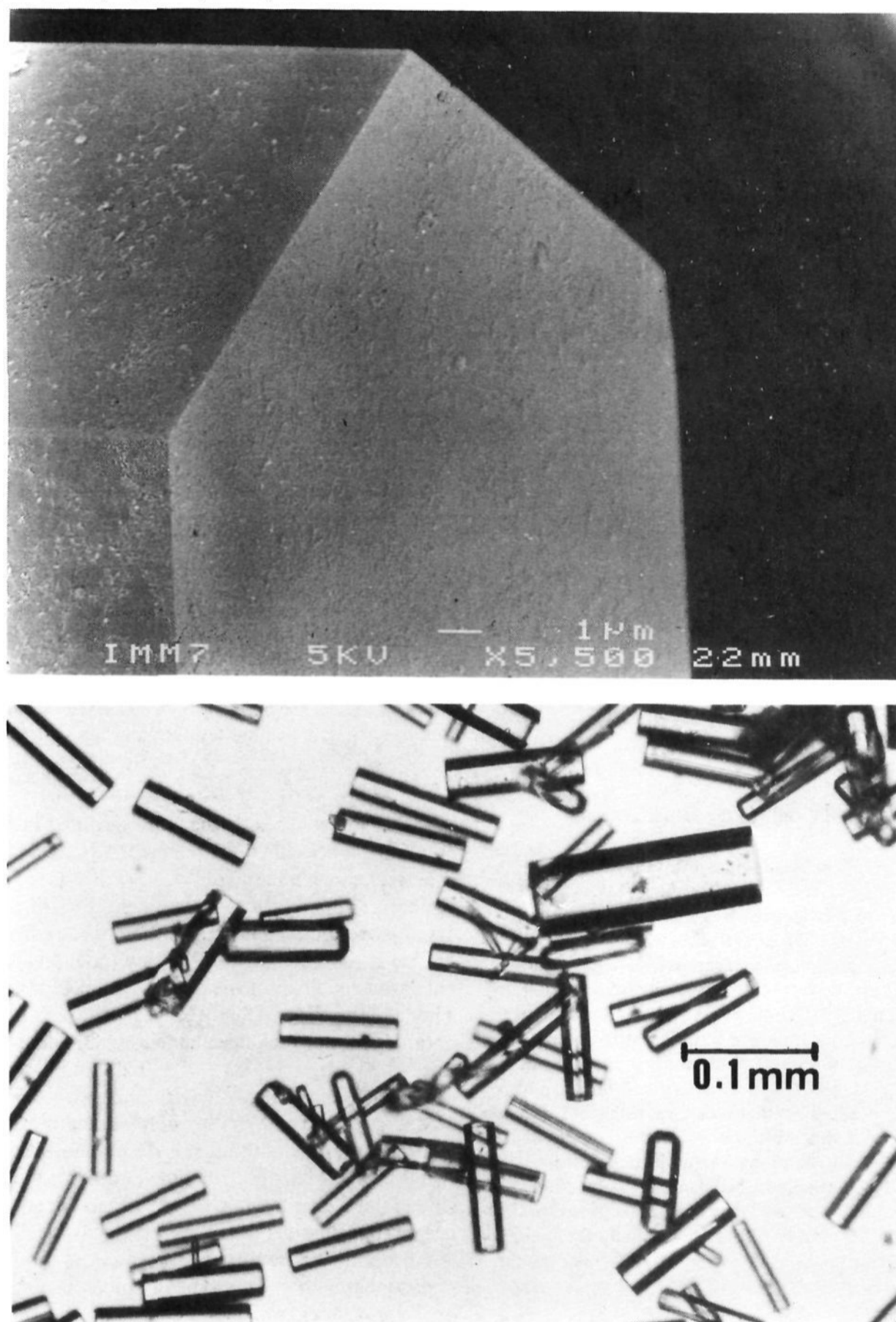


**Figure 2.** (a, top) Scanning electron micrograph of a SAPO-5 crystal showing the smoothness of the surface. (b, bottom) Optical micrograph of SAPO-5 crystals showing the high optical quality.

at 473 K for 90 min are plotted. These conditions are sufficient to remove all adsorbed water, as the flat background between 4000 and 2500  $\text{cm}^{-1}$  proves. For the spectrum labeled  $\theta = 0^\circ$  ( $\theta$  is the angle between the polarization plane of the incident IR radiation and the short axis of the SAPO crystal), the plane of the electric field vector of the IR radiation is oriented perpendicular to the long ( $c$ ) crystal axis;  $\theta = 90^\circ$  indicates that the long crystal axis lies in the polarization plane.

The most striking feature of the spectrum is probably the strong polarization of the OH vibrations at 3627 and 3519  $\text{cm}^{-1}$  (enlarged in the inset in Figure 4). However, also bands in the region of the lattice vibrations below 1200  $\text{cm}^{-1}$  are strongly affected by the polarization of the IR radiation: For the  $c$ -axis of the crystal lying in the polarization plane, bands are observed at 1136, 1000, 951, and 865  $\text{cm}^{-1}$ . For the  $c$ -axis perpendicular to the polarization plane, absorption bands are observed at 992, 934, and 834  $\text{cm}^{-1}$ . Between 1200 and 1000  $\text{cm}^{-1}$ , only the high intensity band at 1136  $\text{cm}^{-1}$  could be identified clearly as a distinct feature in the

broad, very high intensity band, and below 800  $\text{cm}^{-1}$ , the absorption is so high that no evaluation of band positions is possible. This is also due to the increasingly lower signal to noise ratio near the cutoff of the detector at 700  $\text{cm}^{-1}$ .

Slight differences between the differently polarized spectra can also be detected in the spectral region between 2500 and 1200  $\text{cm}^{-1}$ . These effects, however, are much less pronounced and are very difficult to quantify. The bands between 2300 and 2400  $\text{cm}^{-1}$  are due to incomplete compensation of gas-phase  $\text{CO}_2$ .

In order to obtain additional information on the acidity and to assess the orienting properties of the AFI structure, the crystals were in situ loaded with *p*-xylene. Loading at room temperature and at a *p*-xylene pressure of 4.5 Torr proved to be extremely slow. After 3 days, *p*-xylene bands of only low intensity were observed in the IR spectra. Moreover, the leak rate of the cell is too high to retain a good vacuum without pumping over 3 days. Due to the hydrophilicity of the SAPO-5, the crystals were

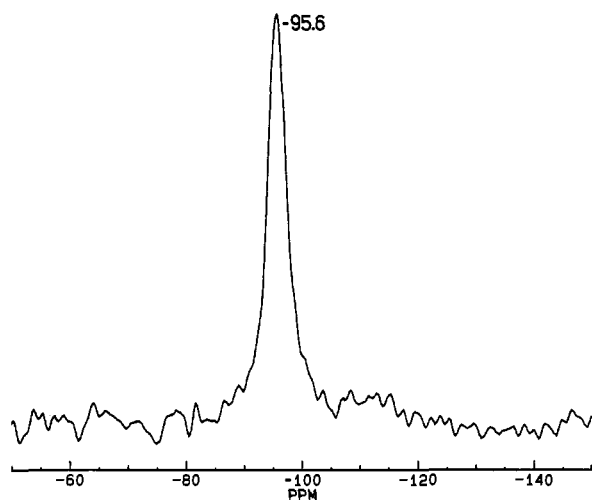
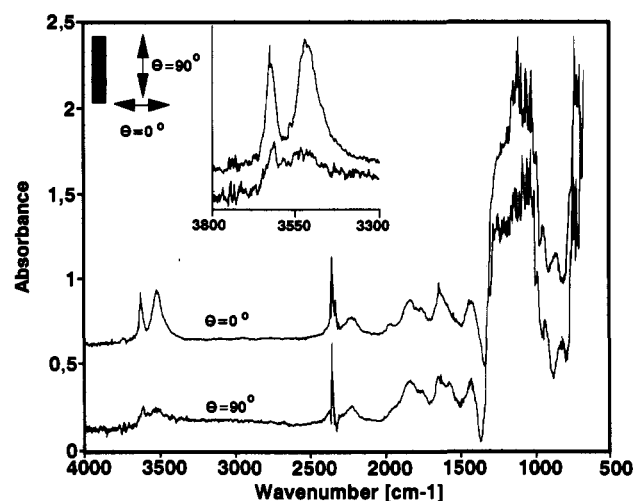
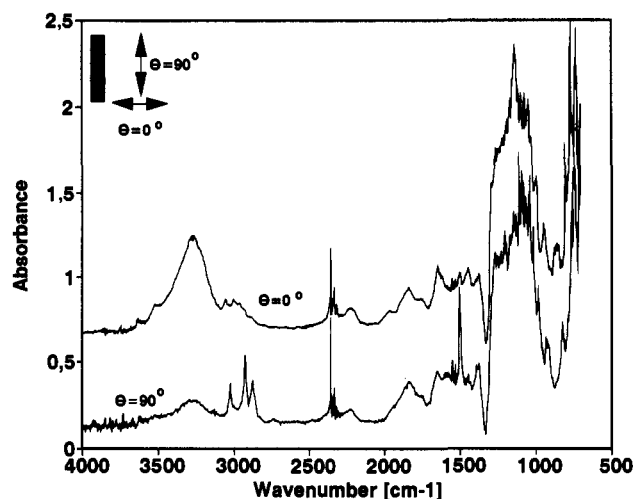
Figure 3.  $^{29}\text{Si}$  MAS NMR spectrum of SAPO-5.

Figure 4. Polarized IR spectra of a SAPO-5 single crystal. Polarization as indicated in the inset, OH region enlarged in the inset.

Figure 5. Polarized IR spectra of SAPO-5 exposed to 4.5 Torr of *p*-xylene for 10 h at 373 K.

partially rehydrated by water vapor which had leaked into the cell. Subsequent loading experiments were thus performed at 373 K. At this temperature saturation of the samples was reached after approximately 6 h. The resulting polarized spectra can be seen in Figure 5. The additional bands found after adsorption of *p*-xylene are listed in Table 2, together with the dichroic ratios and the assignments of the bands.

Table 2. Band Positions, Dichroic Ratios, and Band Assignments<sup>a</sup>

position (cm <sup>-1</sup> )	dichroic ratio (0°/90°)	assignment
3625 <sup>b</sup>	4.3	$\nu\text{OH}$ (12-ring)
3520 <sup>b</sup>	5.3	$\nu\text{OH}$ (6-ring)
3327	6.2	$\nu\text{OH}$ bonded to xylene
3047	~10	?
3025	~0.1	20a
3003	~10	20b
2920	0.07	$\nu_s$ (CH)
2870	0.13	$2\delta_{as}$ (CH)
1519	0.12	19a
805	~5	11

<sup>a</sup> Following Green /24/. <sup>b</sup> Prior to xylene adsorption.

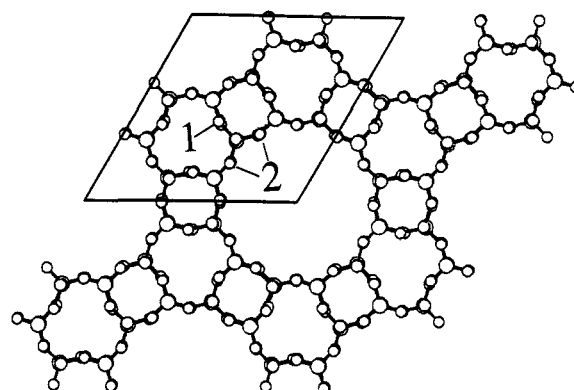


Figure 6. SAPO-5 structure with OH positions in the 6-membered ring (1) and in the 12-membered ring (2).

## Discussion

The spectrum in the OH region—except for the polarization which has not been reported before—is well in accordance with literature data obtained from the analysis of powdered polycrystalline samples, recorded in either transmission or diffuse reflectance. The bands at 3625 and 3519 cm<sup>-1</sup> have been reported by several authors.<sup>15,17,20–23</sup> These bands have been attributed to unperturbed Si–OH–Al groups for the 3625-cm<sup>-1</sup> band and to OH groups in constrained environments, probably in 6-membered rings, for the 3520-cm<sup>-1</sup> band.<sup>15,21,19</sup> Additional bands found by other authors in aluminophosphates at 3675–80 cm<sup>-1</sup><sup>15,19,21,22</sup> (P–OH), 3740–50 cm<sup>-1</sup><sup>15,19,21,22</sup> (SiOH in impurities or in SiO<sub>2</sub> domains of the crystal), and 3790 cm<sup>-1</sup><sup>15</sup> (AlOH) have not been observed in this study. This is probably due to two factors: (1) The spectra are—compared with spectra obtained from polycrystalline powder—relatively noisy due to the low-energy throughput in single crystal studies. Thus low-intensity peaks might vanish in the noise. (2) The crystals are of high quality so that defect sites giving rise to the aforementioned bands are present in low concentration only. At least amorphous silica impurities, intermixed with the polycrystalline SAPO-5 material, which have been suggested as the reason for the 3745-cm<sup>-1</sup> band, are definitely not present in the material studied here, since only the pure SAPO-5 crystal has been selected by the apertures.

The polarization of the bands at 3625 and 3519 cm<sup>-1</sup> observed in the present study indicates that the OH groups associated with the bands are primarily oriented in the *ab*-plane with a mean deviation of about 18°. On inspecting the AFI structure, two possible locations for the OH groups can be identified (Figure 6). One is a bridging O-atom protruding into the 6-ring in the *ab*-plane (position 1 in Figure 6); the other position is a bridging

(20) Halik, C.; Lercher, J. A.; Mayer, H. J. *Chem. Soc., Faraday Trans. 1* **1988**, *84*, 4457–69.

(21) Zscherpel, U.; Staudte, B.; Löffler, E.; Peuker, C.; Jahn, E. *Z. Phys. Chem. (Leipzig)* **1989**, *270*, 207–11.

(22) Hegde, S. G.; Ratnasamy, P.; Kustov, L. M.; Kazansky, V. B. *Zeolites* **1988**, *8*, 137–41.

(23) Martens, J. A.; Grobet, P. J.; Jacobs, P. A. *J. Catal.* **1990**, *126*, 299–305.

O-atom in the 12-ring channel (position 2). These positions would correspond to the band assignments by other authors listed earlier. Other possible locations are fairly improbable, since the T–O–T angle at such positions seems to be close to 180°, which would make these sites energetically unfavorable for the accommodation of an additional negative charge.

Under the assumption that the transition moments of the OH vibrations are oriented along the bond, the angles between the *ab*-plane and the OH bond inferred from the dichroic ratios indicate a hybridization between  $sp^2$  and  $sp^3$  for the charge-bearing oxygen atoms, if a static deviation is assumed. For an  $sp^2$  hybridization, a dichroic ratio of infinity would be expected (or, taking into account the depolarization in the microscope, of about 100), since the OH bond would then lie in the intersection of the T–O–T plane with the *ab*-plane. The fact of a *z*-contribution to the band intensity allows us to conclude a significant  $sp^3$  contribution.

An alternative explanation could be a dynamic deviation of the OH bond from the *ab*-plane, since the OH bending vibration would also give rise to a *z*-contribution to the band intensities. The extent of this dynamic contribution would be dependent on the amplitude of the vibration and on the degree of excitation of this vibration. Temperature-dependent measurements to solve this problem are in progress.

The positions in the 6- and the 12-membered rings had already been earlier connected with the observed IR bands: the 3625- $cm^{-1}$  band had been assigned to an OH group in the main channel,<sup>15,19,21</sup> and the 3520- $cm^{-1}$  band was assigned to an OH group in a 6-membered ring.<sup>15,19,21</sup> The reduced frequency was attributed to additional H-bonding in the 6-membered ring. This conclusion is supported by the polarized spectra. The angle between the OH bond and the *ab*-plane seems to be slightly lower for the group absorbing at 3520  $cm^{-1}$ . This can be explained by the hydrogen bonding which would bond the hydrogen atom closer to the ring plane and thus reduce the deviation of the OH bond from the *ab*-plane.

Additional evidence for this assignment was given in the literature based on benzene sorption experiments. Only the OH group corresponding to the 3625- $cm^{-1}$  vibration was found to react with the large, weakly basic benzene molecule,<sup>19,22</sup> while the band at 3520  $cm^{-1}$  only vanished after exposure to ammonia. In the work of Martens et al.,<sup>17</sup> however, there is an indication of a reaction of the benzene molecule also with the OH group corresponding to the 3520- $cm^{-1}$  vibration. A similar result was obtained in the present study, using *p*-xylene, which is somewhat more basic than benzene. The bands at 3625 and 3520  $cm^{-1}$  are very much reduced, while a broad band at 3233  $cm^{-1}$  with the same polarization as the OH bands appears after exposure to *p*-xylene. The new band at 3233  $cm^{-1}$  probably corresponds to the OH groups which show an unperturbed signal at 3625  $cm^{-1}$ . The band at 3520  $cm^{-1}$  is probably shifted to the same value, since no other band corresponding to these OH groups could be detected. The only other possibility would be a shift to low wavenumbers below 3000  $cm^{-1}$ , where a broad, low intensity background band might be present. However, this broad band is very difficult to analyze and could be due to other effects. Moreover, a shift by almost 600  $cm^{-1}$  into the aliphatic CH region would correspond to an unrealistically high acid strength.

However, this leaves the question unanswered of how the OH group in a 6-membered channel can react with *p*-xylene. An explanation could be that an energetically more favorable position in the 12-ring channel exists, if the OH is bonded to a basic molecule like *p*-xylene. Such an effect could shift the charge and the proton from the position 1 in Figure 6 to position 2 in the 12-ring channel. Since the adsorption experiments were performed at 373 K, a sufficiently high mobility of the proton for this shift can be expected. The band previously located at 3520  $cm^{-1}$  would appear after reaction with the base at the same position as the band previously located at 3625  $cm^{-1}$ , because after reaction

with the base both OH groups would be in identical positions in the 12-ring channel. This explanation would also account for the relatively large intensity of the 3233- $cm^{-1}$  band as compared to the individual OH bands prior to xylene adsorption. The discrepancy to the work of Halik et al.<sup>20</sup> and Hegde et al.<sup>22</sup> could be due to their use of benzene, which is less basic than xylene and thus only gives rise to a smaller energetic effect. This is supported by the work of Zibrowius et al.,<sup>18</sup> who observed a reaction of *both* types of OH groups with the strong base pyridine, which is in size comparable to benzene. These findings indicate that great care should be exercised in using the term "accessibility" of groups in molecular sieves. This term usually suggests a steric accessibility. One should, however, keep in mind that in a dynamic system an energetic preference for the formation of a certain complex might lead to changes in atomic positions. Such a relaxation process could allow the reaction between groups which would, due to steric restrictions, not occur if the system were static.

The *p*-xylene molecules themselves are well aligned in the SAPO-5 channel. The high dichroic ratios of all *p*-xylene bands show that the deviation of the long axis of the molecule from the SAPO-5 *c*-axis is about 10°. Band assignment is possible without ambiguity, as given in Table 2. As in the case of *p*-xylene in silicate I,<sup>12</sup> the band at 3050  $cm^{-1}$  could not be assigned. This band is probably a combination band. Another possible explanation would be a distortion of the *p*-xylene in the pore system which lowers the symmetry and in turn allows vibration 2 to become IR active, which is normally only Raman active. This explanation, however, can be ruled out by the parallel polarization of the observed band, whereas vibration 2 should be perpendicularly polarized. Altogether, the spectra show less features than in the case of *p*-xylene in silicate I.<sup>12</sup> This is due to the fact that the SAPO-5 spectra have a worse *S/N* ratio, thus showing only the high-intensity bands.

A band at 805  $cm^{-1}$  could be observed for *p*-xylene in SAPO-5 which was blanked out by strong lattice vibrations in the case of silicalite. This band can be assigned to vibration 11 following the nomenclature of Green.<sup>24</sup> This vibration is a  $B_{3u}$  species with the expected polarization being parallel.

Although the *p*-xylene molecules are well aligned in the SAPO-5 crystal, the question remains whether the preferred orientation of the OH groups in the SAPO-5 in turn orients the *p*-xylene molecules, or whether it is the channel structure itself. Since the silicon content of the material is relatively high, the crystal channel system is probably filled to a large extent already when all the OH groups have reacted with xylene. Since the OH groups are highly oriented, this would lead to an orientation of the *p*-xylene perpendicular to the OH groups, since it is the benzene ring plane reacting as the basic part of the molecule. The NMR spectrum proved the almost perfect incorporation of silicon onto phosphorus sites of the lattice, surrounded by four aluminum atoms.<sup>17,19,23,25</sup> There is thus a sufficient number of OH groups to coordinate a major part of the *p*-xylene molecules. A possible way to study the effect of the channel system of the AFI structure alone would be the analysis of *p*-xylene-loaded  $AlPO_4-5$  crystals or SAPO-5 with a much lower silicon content. However, so far we have not succeeded in synthesizing such materials with the necessary optical quality for the IR-microscopic analysis.

## Conclusion

Using FTIR microscopy in connection with a newly constructed HV cell, we were able to obtain spectra of SAPO-5 single crystals for the first time. One prerequisite, the availability of SAPO-5 crystals with a high optical quality, was met by developing a well-tuned synthesis procedure. <sup>29</sup>Si MAS NMR spectroscopy

(24) Green, J. H. S. *Spectrochim. Acta* 1970, 26A, 1503–13.

(25) Martens, M.; Martens, J. A.; Grobet, P. J.; Jacobs, P. A. In *Guideline for Mastering the Properties of Molecular Sieves*; Barthomeuf, D., et al., Eds.; Plenum Press: New York, London, 1990; pp 1–51.

established the almost perfect incorporation of silicon onto phosphorus sites in the lattice.

Since the use of single crystals allows orientation of the material with respect to the IR beam, polarized spectra could be recorded to obtain additional structural information. The OH groups were found to be primarily oriented in the *ab*-plane, probably protruding in the 12-membered main channel and the parallel 6-membered ring channels, respectively. Both kinds of OH groups reacted with *p*-xylene, the OH groups in the 6-membered ring channel probably being forced into the main channel by this reaction. Either due to the orientational effect of the OH groups or due to the channel system, the xylene molecules are also highly

oriented, i.e. the long molecule axis lies primarily in the direction of the AFI *c*-axis. This demonstrates again the potential of the AFI structure to macroscopically orientate absorbed guest molecules, a property which has already been exploited for the strong SHG from *p*-nitroaniline-loaded  $\text{AlPO}_4\text{-5}$ .

**Acknowledgment.** Financial support by the DFG under Grant No. Schu 744/4-1, by the Fonds der Chemischen Industrie, and by the BMFT is gratefully acknowledged. We would also like to thank K. Unger, R. A. van Santen, and A. Monnier for helpful discussions and U. Ritzler (IMM Mainz) for the electron microscopic analysis.